Manipulation of the nanoscale presentation of integrin ligand produces cancer cells with enhanced stemness and robust tumorigenicity

Siu Hong Dexter Wong,[†,‡,⊥] Xiao Xu,[ξ,⊥] Xi Chen,[†,ζ,⊥], Ying Xin,[†,ζ] Limei Xu,[ξ] Chun Him Nathanael Lai,[‡] Jiwon Oh,[‡] Wai Ki Ricky Wong,[‡] Xuemei Wang,[‡] Shisong Han,[‡,ǁ,ǂ], Wenxing You,[‡,∀] Xintao Shuai,[ǁ,ǂ] Nathalie Wong,[‡,∀] Youhua Tan,[†, ζ,*] Li Duan,[ξ,*] Liming Bian[‡,▽,Δ,*]

[†]Department of Biomedical Engineering, The Hong Kong Polytechnic University, Hong Kong, 999077, China; [‡]Department of Biomedical Engineering, The Chinese University of Hong Kong, Hong Kong, 999077, China; [ζ]The Hong Kong Polytechnic University Shenzhen Research Institute, Shenzhen, China; [ξ]Department of Orthopedics, Shenzhen Intelligent Orthopaedics and Biomedical Innovation Platform, Guangdong Artificial Intelligence Biomedical Innovation Platform, Shenzhen Second People's Hospital, the First Affiliated Hospital of Shenzhen University Health Science Center, Shenzhen, 518035, China; [ǁ]PCFM Lab of Ministry of Education, School of Materials Science and Engineering, Sun Yat-sen University, Guangzhou, 510275, China; [ǂ]Laboratory of Interventional Radiology, Department of Minimally Invasive Interventional Radiology, and Department of Radiology, the Second Affiliated Hospital of Guangzhou Medical University, Guangzhou, 510260, China; [∀]Department of Surgery at Sir Y. K. Pao Centre for Cancer, The Chinese University of Hong Kong, Hong Kong, 999077, China; [▽]Shenzhen Research Institute The Chinese University of Hong Kong, Shenzhen, 518172, China; [Δ]China Orthopedic Regenerative Medicine Group (CORMed) Hangzhou, Zhejiang, 310058, China

[⊥]These authors contributed equally

***Corresponding Author:**

Youhua Tan: youhua.tan@polyu.edu.hk

Li Duan: duanl@szu.edu.cn

Liming Bian: lbian@cuhk.edu.hk

Keywords: Cancer Stem-like Cells, Magnetic Actuation, Nanoscale Tether Mobility, Tumour Mechanobiology, Ligand Presentation

Abstract

Developing strategies for efficient expansion of cancer stem-like cells (CSCs) *in vitro* will help investigate the mechanism underlying tumorigenesis and cancer recurrence. Herein, we report a dynamic culture substrate tethered with integrin ligand-bearing magnetic nanoparticles via a flexible polymeric linker to enable magnetic manipulation of the nanoscale ligand tether mobility. The cancer cells cultured on the substrate with high ligand tether mobility develop into large semi-spherical colonies with CSCs features, which can be abrogated by magnetically restricting the ligand tether mobility. Mechanistically, the substrate with high ligand tether mobility suppresses integrin-mediated mechanotransduction and histone-related methylation, thereby enhancing cancer cell stemness. The culture-derived high-stemness cells can generate tumours both locally and at the distant lung and uterus much more efficiently than the low-stemness cells. We believe that this magnetic nano-platform provides a promising strategy for investigating the dynamic interaction between CSCs and the microenvironment and establishing a cost-effective tumour spheroid model.

Introduction

Despite the advance in cancer therapeutics and improved survival rate of cancer patients, tumour recurrence remains a significant challenge in clinical practice[1-5] and is believed to arise from a small subpopulation of cancer stem-like cells (CSCs). These cells are resistant to chemo-/radio-therapy and highly malignant, and can induce cancer recurrence.[6-7] Therefore, characterizing CSC properties and elucidating their high malignancy mechanisms are critical for developing effective anticancer therapies. Due to the rarity within a heterogeneous tumour, the isolation and cultivation of CSCs are essential for functional characterization and mechanistic studies.[8] However, the existing methods to isolate CSCs from primary cancer tissues, such as flow cytometry, are costly and inefficient.[9] Developing strategies including non-adhesive surfaces and hanging droplets for generating multicellular cancer spheroids as *in vitro* models of solid tumours has become an active area of research.[10] However, these strategies often rely on suspension-induced cell aggregation and have limited control over the formed cancer spheroids. Some reports showed that low-stemness cancer cells seem to spontaneously and stochastically turn into CSCs *de novo*,[11,12] and conventional strategies provide limited information underlying molecular mechanism of CSCs plasticity.

Except for genetic and biochemical factors, mechanical forces play important roles in tumour growth and metastasis because cells can sense and respond to mechanical cues through mechanotransduction.[4,9] Specifically, cells sense matrix rigidity through mechanosensors such as integrin-mediated signalling molecules, including focal adhesion kinase (FAK), Ras homologue family member A (RhoA) and cell division control protein 42 homolog (Cdc42), to initiate mechanotransduction signalling.[12-14] Recent studies have suggested that cell-adhesive matrice rigidity epigenetically regulates cancer cell behaviour *via* FAK signallings.[15-17] These findings indicate that regulating the interaction between cells and the microenvironment critically influences cellular responses. Thus, previous works have demonstrated the application of dynamic platforms to investigate and regulate cell–microenvironment interactions. For instance, an optically controlled culture substrate based on merocyanine-to-spiropyran isomerization was reported to switch the ligand presentation between diffusible state and constant state reversibly to regulate integrin-dependent stem cell adhesion and differentiation.[18] Such platform further demonstrated that cells rely on $\alpha_5\beta_1$ integrin-mediated Rac signalling for the early adhesion stage (diffusive ligands) and develop self-strengthening adhesive force through $\alpha_v\beta_3$ integrin-mediated RhoA/ROCK signalling for the latter adhesion stage (constant ligands).[19] Also, we have previously developed platforms to regulate the mechanosensing of seeded cells and the associated signallings *via* modulating integrin-ligand binding dynamics.[20-24] We thus believe that it is possible to cultivate

CSCs by using dynamic platforms to manipulate the cancer cell-substrate interactions.

In this study, we describe a dynamic culture substrate consisting of integrin ligand-bearing magnetic nanoparticles (RGD-MNPs) conjugated to a glass substrate *via* flexible and non-fouling poly(ethylene) glycol (PEG) linkers with varying molecular weights (MW: 2k, 5k, and 20k Da) according to our previous report (Scheme 1).[21] Unlike anhydrides, ester, and amides groups, PEG is generally considered much less susceptible to hydrolytic degradation and is non-biodegradable, which can be used to passivate nanoparticles or drugs to extend the half-life of blood circulation.[25] Also, it has been utilized as a cellular traction force sensor due to its ability of reversible folding/unfolding at resting/stretching state.[26,27] We hypothesize that this platform can dynamically alter the cellular integrin-based mechanosensing and epigenetic profile that regulate the stemness of the cultured cancer cells. Recent work has utilized matrix (e.g., collagen-coated polyacrylamide gel) stiffness as a biophysical parameter, especially substrate softness, to study the effect of receptor-ligand mediated self-renewal behaviour of cancer cells and embryonic stem cells.[28,29] It should be noted that the deformability of the collagen can be subject to the number of collagen-matrix anchoring points (e.g., the pore size of the matrix network and the nanospacing of ligands tether) that create a local matrix stiffness.[30,31] This local mechanical property can be different from that of the bulk matrix and therefore generating potential confounding factors. In this platform, we precisely controlled the coating density and adjusted the tether length (MW of the PEG) of cell adhesive ligand on the same rigid glass substrate, and this help decouples the effects of local rigidity from that of bulk substrate mechanical properties. We believe that the large or small molecular weight of the PEG linkers, i.e., high or low RGD tether mobility, can produce effects similar to that of the "soft" or "stiff" substrate, respectively. In this study, we showed that the cancer cell lines and patient cancer cells cultured on the substrate with high-mobility of RGD-MNPs demonstrated CSC attributes, including enhanced colonial expansion, stemness markers expressions, drug resistance, and *in vivo* tumorigenicity and metastasis. We further showed that the high-mobility of RGD tether suppressed mechanotransduction signalling in cancer cells and histone-related methylation, thereby promoting stemness and the associated behaviours. We believe that this magnetic-controlled system provides an effective tool for fundamental and preclinical research for anticancer therapy.

Results and discussion

We first fabricated monodispersed silica-coated MNPs (core size: 10.9±0.8 nm, silica-coated size: 28.3±2.0 nm) (Figure 1a). We performed dynamic light scattering to determine the size of the MNPs, Fourier transform infrared spectroscopy to characterize the successful conjugation of RGD

to MNPs, and vibrating-sample magnetometry and x-ray diffraction to confirm the magnetic properties of the as-prepared MNPs (Figures S1-3). We confirmed this dynamic substrate consisted of a monolayer of RGD-MNPs grafted on a glass substrate with controlled particle densities (460±11 particles/μm^2) through PEG linkers of varying MWs (Figure 1a), with narrow conjugated-RGD density (263±30 peptides/particle). In this study, we hypothesized that increasing the PEG MW enhances the tether mobility of the RGD-MNPs and suppresses the mechanosensing of the seeded cells in the absence of downward magnetic attraction (–M), thereby mimicking a "soft substrate". Switching on the downward magnetic attraction (+M) restricts the tether mobility of the RGD-MNPs, mimicking a "stiff substrate" and enhances the mechanosensing of the cells. Such restricted and unleashed tether mobility *via* magnetic actuation enables effective switching between different biophysical states of the dynamic substrate, regulating cancer cell mechanosensing and cellular functions. All experimental and control group abbreviations are listed in Table 1.

We performed atomic force microscopy (AFM) analysis to verify the magnetic actuation of our platform (Figure 1b and c). In contact mode, most conjugated RGD-MNPs in all groups were swiped away from the cantilever scanning region in –M (Figure 1b). In contrast, fewer particles were removed from the substrate under +M (Figure 1c), suggesting that the RGD-MNP tether mobility can be restricted magnetically. To quantify the tether mobility of RGD-MNPs with increasing PEG linker MW, we estimated the nano-movement of the tethered RGD-MNPs by AFM in tapping mode with immobilized gold nanorods as reference points (Figure 1d & S4). The difference in the relative coordinates of the RGD-MNPs before and after lateral magnetic attraction shows that MNP20k exhibited the largest relative displacement (63.9±13.4 nm) compared to MNP5k (15.3±5.5 nm) and MNP2k (7.9±2.8 nm), which correlate well to the theoretically extended chain lengths of PEG with MW 20kDa (161.8 nm), 5kDa (38.2 nm) and 2kDa (17.8 nm), respectively.[32,33] These results indicate that increasing the PEG linker MW from 2-20 kDa enhances RGD-MNP tether mobility, i.e., decreasing rigidity of the tether structure. In contrast, the random RGD-MNP movement (–M) did not significantly influence the RGD-MNP displacement quantification, probably due to the collapsed and coiled conformation of the PEG without tension at resting state (Figure S5).[26] These results demonstrate that our dynamic substrate offers flexible control over the ligand tether mobility, depending on the PEG linker length and magnetic actuation.

We next tested the effect of the dynamic substrates on tumour cell behaviours. Single HeLa cells on the substrates with increasing ligand tether mobility grew into semi-spherical tumour spheroids (Figure S6b), especially in the MNP20k–M group, which showed the highest number of

colony formation and the largest colonies over 7 days of culture (Figure S6c-f & S7b). However, cells on substrates with intrinsically low or magnetically restricted ligand tether mobility barely grew into colonies but a cell monolayer with significant cell spreading (Figure S6a, c-f & S7a). Besides, increasing the initial cell seeding density did not significantly enhance the cell colony formation by cell aggregation, and cells remained a cell monolayer in the MNP20k+M group (Figure S8). These findings suggest that tether mobility is the key factor in regulating the formation of the multicellular tumour semi-spheroid colonies by HeLa cells.

We further evaluate the plasticity of tumour cells in response to varied mechanical microenvironments. The HeLa cells cultured on the MNP20k–M substrate showed an increased number of semi-spherical colonies in the first 3 days, which became flattened as a cell monolayer in the next 4 days after the MNP20k–M substrate switching to MNP20k+M (Figure S7c). This property of tunable nanoscale presentation of integrin-ligands is potentially a unique advantage of our platform, which is not available from conventional methods for supporting tumour spheroid growth. Consistent with the findings in HeLa cells, other adherent cancer cell lines, including MCF-7, MDA-MB-231, Hep3B, murine B16-F1, and primary human colon cancer cells, all developed semi-spherical colonies on the MNP20k–M substrate over 7 days (Figure S9). Furthermore, HeLa cells cultured on the substrates with MNPs bearing no RGD or non-bioactive RAD (+/–M) only resulted in sparse small cell aggregates, which were drastically different from the large colonies from the MNP20k–M group (Figure S10a, c-e). We also evaluated the conventional agarose substrate, which has no specific interactions with the cells, for supporting the clonal growth of cancer cells.[34] HeLa cells cultured on the agarose substrate developed less regular colonies in morphology and much smaller in size than the colonies derived from the MNP20k–M substrate (Figure S10b-e). These results demonstrate that a basal level of integrin-ligand interaction is required for the survival and expansion of cancer cells[35], and our strategy provides a generalized method for supporting the clonal expansion of a wide array of adherent cancer cells. Importantly, our results indicate that manipulating cell-substrate interactions is an effective approach to enhance the colony growth of cancer cells.

We next investigated the influence of the magnetically controllable tether mobility of the RGD-MNPs on the mechanotransduction signalling of HeLa cells that might contribute to the as-mentioned differential cellular responses. Cytoskeleton components (e.g., F-actin) and mechanosensitive signalling factors such as FAK and Cdc42 are known to be involved in the response of living cells to mechanical stimulations.[17,36] Immunofluorescence staining showed that the expressions of these components decreased on the substrates with increasing tether mobility (MNP2-20k–M) (Figure 2a). In contrast, cells cultured on the substrate with low/magnetically

restricted ligand tether mobility (MNP2-20k+M) showed robust expression of these mechanotransduction markers. Consistently, the western blot data showed the same trend in the expressions of total and phosphorylated FAK, Cdc42 and RhoA (Figure S11). Hence, the results reveal that high-mobility of the ligand tether suppresses mechanotransduction signalling in cancer cells, and magnetically restricted ligand tether mobility rescues this effect.

Previous studies have shown that FAK activity is closely associated with histone H3 lysine 9 methylation (H3K9me),[17] which is known to repress the expression of stemness-related markers, including Sox2, Nanog and Oct3/4.[37] Our data showed that HeLa cells cultured on MNP20k–M substrate expressed the lowest levels of H3K9me2&3, which potentially contributed to the pronounced expression and nuclear localization of Sox2, Nanog, and Oct3/4 (Figure 2a-d & S12). However, cells cultured on low or magnetically restricted ligand tether mobility substrate showed high levels of H3K9me2&3 and reduced expression of stemness-related markers. Furthermore, the gene expressions of the stemness-related markers exhibited the same trend at the mRNA level (Figure 2c-e). Our EdU cell proliferation assay showed that the number of HeLa cells undergoing DNA replication in the MNP20k–M group was 131±45% higher than that of the MNP20k+M group (Figure S13). This result is consistent with the profound expression of Sox2, which may positively correlate with cancer cell division.[38] Contrarily, although tumour cells can grow into tumour colonies to a certain extent on agarose substrates, Sox2 was sparsely expressed in the cells within the colony on agarose substrates, different from the cells cultured on the MNP20k–M substrate (Figure S14). These findings suggested that high-mobility of the RGD-MNPs tether enhances the colony growth and stemness of HeLa cells by elevating the associated epigenetic activities.

To confirm the role of mechanotransduction signalling in regulating cancer cell stemness, we showed that knockdown of FAK, Cdc42, or RhoA with the corresponding siRNA increased colony formation, expression and nuclear localization of Sox2 and Nanog in HeLa cells cultured on MNP20k+M substrate (Figure S15a-c). Inhibiting these gene expressions had no obvious effects on the cells cultured on MNP20k–M substrate. However, the inhibition of β_1- integrin inhibited the clonal growth and stemness of HeLa cells even on MNP20k–M substrate (Figure S15d). The results suggest that a basal β_1 integrin-mediated activity is needed for the clonal growth of cancer cells on the substrate with varying RGD-MNP tether mobilities.[39]

We also examined the expression of stem cell surface markers, including CD44 and CD133, which are generally enriched in CSCs and positively correlated with Sox2 and Oct3/4.[40-42] Strikingly, the flow cytometry data indicated that the percentages of the cells expressing CD44 and

CD133 in the MNP20k–M group were 99.93% and 17.99%, respectively, after 7 days of culture (Figure S16e). In comparison, only 0.8-1.54% and 1.66-2.6% of cells in the low/restricted ligand tether mobility groups expressed these two markers (Figure S16a-d). We question whether the dominant population of the high-stemness cancer cells from the MNP20k–M group resulted from selecting high-stemness subpopulation cells or conversion from cancer cells with initial low-stemness. We performed fluorescence-activated cell sorting of $CD44^+/CD133^+$ or $CD44^-/CD133^-$ cells from regular HeLa cells and cultured the sorted cells in different conditions (Figure 3a-b). Intriguingly, 20.6% of the $CD44^+/CD133^+$ cells maintained the expression of both markers after 7 days of culture on the MNP20k–M substrate (Figure 3c), but only 3.53% and 4.40% of $CD44^+/CD133^+$ cells remained on glass and MNP20k+M substrate, respectively. More importantly, our results showed that 17.32% of initially $CD44^-/CD133^-$ cells acquired positive expression of CD44 and CD133 on the MNP20k–M substrate (Figure 3d). In contrast, nearly no cells cultured on the glass/MNP20k+M substrates expressed these markers. The high expression of Nanog in MNP20k–M substrate-derived cells may contribute to the acquired expression of the surface markers.[43]

We further used aphidicolin (DNA replication inhibitor) to rule out selected growth of a high-stemness subpopulation on the dynamic substrate. HeLa and Hep3B cells cultured in different conditions for 1-day without drug exhibited limited stemness marker expressions (Figure 3e & S17a), suggesting that the seeded cells had not developed significant CSC characteristics after only 1-day of culture. Subsequently, cells cultured on both the MNP20k+/–M substrates with the drug for 7-days mostly remained isolated single cells with minimal proliferation (Figure 3f & S17b). However, only cells cultured on the MNP20k–M substrate acquired upregulated expression of Nanog, CD44 and CD133 regardless of the drug treatment (Figure 3f-i & S17b-c). We further demonstrated that primary human colon cancer cells acquired high-stemness with a similar trend as the HeLa cells (Figure S17d-f), although the cells had pre-existing high expression level of $CD44^+/CD133^+$ expression (20-40%) on 1-day of culture, consistent with the elevated expression of stemness markers in colon cancer cells reported previously.[44] These findings show that our dynamic culture substrate can enhance cancer cell stemness and maintain this characteristic in cancer cells with an initial high-stemness level. Thus, this platform can be highly instrumental in investigating the impact of microenvironmental biophysical cues on the plasticity of CSCs

To evaluate the malignancy of tumour cells cultured on the substrates with varying ligand tether mobilities, we next tested their drug resistance ability to doxorubicin, 5-fluorouracil, and gefitinib at different concentrations (Figure S18).[45,46] Importantly, cells cultured from the MNP20k–M substrate exhibited higher chemoresistance ability than cells in other groups at

varying drug dose (Figure S18a-e). We examined the expressions of drug resistance genes, such as ATP-binding cassette superfamily G member 2 (ABCG2) and multidrug resistance transporter (MDR) protein[47], that are known and responsible for the efflux of the drugs out of tumour cells (Figure S18f).[48,49] Strikingly, the expression levels of both ABCG2 and MDR1-3 in the MNP20k–M group were significantly higher than those in the MNP2-5k–M and MNP2-20k+M group after 7 days of culture. These findings demonstrate that tumour cells cultured on the substrates with high ligand tether mobility exhibit enhanced drug resistance.

Evidence revealed that cells were able to develop mechanical memory of the past exposure to physical signals.[50,51] This mechanical memory was shown to be reversible or irreversible, depending on the mechanical dosing (incubation period) on particular matrix stiffness. This priming of cells by a given matrix stiffness influenced their future differentiation and cell migration on a different matrix. Thus far, in our study, this is highly possible that cancer cells primed with high ligand tether mobility retained the memory of such biomechanical environment in vitro with the acquired cancer stem-like cell features in subcutaneous space or during the blood circulation upon injection and hence exhibited robust tumorigenicity and metastasis. To create a melanoma model, we choose a typical murine skin cancer cell line, B16-F1 cells, for evaluating the tumorigenicity of cancer cells primed from our platform *via* subcutaneous injection of these cells into immunocompetent BALB/c mice.[52] Strikingly, cells from MNP20k–M group developed tumours 7-9 times larger in size than those generated by the cells from glass/MNP20k+M substrates (Figure 4a-b) 2 weeks after injection. Tumours from the MNP20k–M group showed the highest tumour cell density, whereas tumours from the glass substrate/MNP20k+M group had loosely packed tumour cells (Figure 4a & c). Since the injection of foreign cells can trigger the host immune response in BALB/c mice,[53] we further examined the expression of programmed death-ligand 1 (PD-L1), which is known to increase the survival and aggressiveness of cancer cells *in vivo*.[54,55] MNP20k–M group-derived tumours had a significantly higher percentage of PD-L1-positive cells than those from the glass substrate/MNP20k+M groups (Figure 4a & d). Moreover, only cells in the tumours from the MNP20k–M group expressed high nuclear localization of Sox2 (Figure 4a & e), which has been reported to regulate the expression of PD-L1.[56] However, our *in vitro* results show that both B16-F1 and HeLa cells cultured on the MNP20k+/–M substrate did not spontaneously express PD-L1 for 7 days (Figure S19a & c), possibly due to the lack of interferon (IFN) secreted by activated immune cells in the tumour environment.[57] To test this possibility, we stimulated both HeLa and B16-F1 cells cultured on the MNP20k+/–M substrate, respectively, with IFN-γ for 1 additional day. The cells in MNP20k–M group exhibited intense expression of PD-L1; weak PD-L1 expression was observed in cells from the MNP20k+M group (Figure S19b & d). These results suggested that high RGD tether mobility substrate-cultivated

cancer cells acquire strong immunoresistance ability, which may facilitate tumour growth *in vivo*.

To create a lung or internal organ metastasis model, we choose a typical cervical cancer cell line, HeLa cells, for evaluating whether ligand tether ligand mobility regulates the metastatic potential of cancer cells.[58] The transwell invasion assay showed that HeLa cells from the MNP20k–M group exhibited significantly enhanced invasion ability than the cells from the low/restricted ligand tether mobility groups (Figure S20). We further injected the HeLa cells ($1x10^5$ cells) from different culture conditions *via* the tail vein of BALB/c mice for establishing a metastasis model. After 1-month, only cells from MNP20k–M group generated metastatic tumours in the lung and uterus of all animals with abnormal morphology (3/3) (Figure 4f-g, S22a-b & g). The tumour cells occupied most alveoli spaces in the lungs and induced significant angiogenesis in the uterus, with high expression of CD44 and CD133 (Figure 4f, h-i & S22c-d, h-i) and cytokeratin 19, a cancer cell marker (Figure S21a & S22e). In contrast, the cells cultured from MNP20k+M/glass substrate did not significantly form any metastatic tumours in the lungs and uterus (both 0/3). Furthermore, the metastatic lung and uterus tumours from the MNP20k–M group harboured a significant amount of PD-L1-positive cells (Figure 4j, S21b, S22f & j), which were absent in the organs from control or glass/MNP20k+M groups. These results suggested that cancer cells cultured on the substrate with the high ligand tether mobility possess high metastatic potential and immunoregulation capability, as typically observed in CSCs.[59]

In summary, our dynamic substrate offers a physical and noncontact strategy (magnetic actuation) to study the effect of the nanoscale presentation of integrin-binding ligands on cancer cell behaviours (Figure S23). In this study, a substrate with high-mobility of ligands effectively generated high-stemness cancer cells from different cancer cell lines or primary patient cancer cells. We demonstrated that our dynamic substrate regulates integrin-based signalling and associated epigenetic events with converting low-stemness cancer cells into high-stemness ones. The obtained high-stemness cancer cells show similar critical traits to those of CSCs in drug resistance and high malignancy. We believe that this culture system with easy imaging access can be a valuable and cost-effective tool to assist basic studies on the plasticity and molecular mechanisms of CSCs behaviour for developing anticancer therapies.

Acknowledgements

S.H.D.W, X.X. and X.C. contributed equally in this study. Project 31570979 is supported by the National Natural Science Foundation of China. This work is supported by General Research Fund Grants from the Research Grants Council of Hong Kong (Project Nos. 14205817 and 14204618); the Health and Medical Research Fund, the Food and Health Bureau, the Government of the Hong Kong Special Administrative Region (Reference No.: 04152836); the Chow Yuk Ho Technology Centre for Innovative Medicine, The Chinese University of Hong Kong; Research Impact Fund from the Hong Kong Research Grants Council (Ref. No.: R4017-18); the National Natural Science Foundation of China (No. 81772394); the Key Program of the Natural Science Foundation of Guangdong Province (No.2018B0303110003); the Shenzhen Science and Technology Projects (No. KQTD20170331100838136; No. JCYJ20170817172023838; No. JCYJ20170306092215436; JCYJ20170413161649437); and the Shenzhen Fund for Guangdong Provincial High-level Clinical Key Specialties (No. SZGSP007). Y.T. acknowledges the support from National Natural Science Foundation of China (Project no. 11672255), Shenzhen Science and Technology Innovation Commission (Project no. JCYJ20170413154735522), and Early Career Scheme from Research Grants Council of the Hong Kong Special Administrative Region, China (PolyU 252094/17E).

Supporting Information

Materials and experimental sections; DLS, FTIR and VSM of functionalized MNPs; TEM and Uv-vis of AuNRs; AFM of the dynamic substrate without magnetic field; optical images with statistical quantification of HeLa cells in different conditions over 7 days; 2D and 3D images of HeLa cell colonies; SEM images of HeLa cell with varies initial cell seeding density; optical images with statistical quantification of different cell lines/types in different conditions; HeLa cell responses on agarose substrates vs our dynamic substrates; quantification of western blots; quantification of nuclear localization of stemness markers; Edu cell proliferation assay; Sox2 staining of HeLa cells cultured on agarose and our dynamic platform; siRNA knockdown assay; flow cytometry for CD44&CD133 expression; aphidicolin treatment assay; drug resistance analysis; examination of PD-L1 expression in vitro; transwell invasion assay; immunostaining of PD-L1 and cytokeratin 19 in lungs; metastatic potential study of HeLa cells in uterus; schematic summary of our study.

Competing interests

The authors declare no competing interests.

References

(1) Dean, M.; Fojo, T.; Bates, S. Tumour stem cells and drug resistance. *Nat. Rev. Cancer* **2005,** *5* (4), 275–284

(2) Baumann, M.; Krause, M.; Hill, R. Exploring the role of cancer stem cells in radioresistance. *Nat. Rev. Cancer* **2008,** *8* (7), 545.

(3) Amos, S. M.; Duong, C. P. M.; Westwood, J. A.; Ritchie, D. S.; Junghans, R. P.; Darcy, P. K.; Kershaw, M. H. Autoimmunity associated with immunotherapy of cancer. *Blood* **2011,** *118* (3), 499–509

(4) Chen, Q.; Wang, C.; Zhang, X. D.; Chen, G. J.; Hu, Q. Y.; Li, H. J.; Wang, J. Q.; Wen, D.; Zhang, Y. Q.; Lu, Y. F.et al. In situ sprayed bioresponsive immunotherapeutic gel for post-surgical cancer treatment. *Nat. Nanotech.* **2019,** *14* (1), 89–97

(5) Liu, J. J.; Chen, Q.; Feng, L. Z.; Liu, Z. Nanomedicine for tumor microenvironment modulation and cancer treatment enhancement. *Nano Today* **2018,** *21*, 55–73

(6) Clara, J. A.; Monge, C.; Yang, Y.; Takebe, N. Targeting signalling pathways and the immune microenvironment of cancer stem cells - a clinical update. *Nat. Rev. Clin. Oncol.* **2019**, 17 (4), 204–232

(7) Visvader, J. E.; Lindeman, G. J. Cancer Stem Cells: Current Status and Evolving Complexities. *Cell Stem Cell* **2012,** *10* (6), 717–728

(8) Wu, L.; Ji, H. W.; Guan, Y. J.; Ran, X.; Ren, J. S.; Qu, X. G. A graphene-based chemical nose/tongue approach for the identification of normal, cancerous and circulating tumor cells. *NPG Asia Mater.* **2017,** *9*, e356

(9) Lee, J.; Kotliarova, S.; Kotliarov, Y.; Li, A. G.; Su, Q.; Donin, N. M.; Pastorino, S.; Purow, B. W.; Christopher, N.; Zhang, W.et al. Tumor stem cells derived from glioblastomas cultured in bFGF and EGF more closely mirror the phenotype and genotype of primary tumors than do serum-cultured cell lines. *Cancer Cell* **2006,** *9* (5), 391–403

(10) Li, Y.; Kumacheva, E. Hydrogel microenvironments for cancer spheroid growth and drug screening. *Sci. Adv.* **2018,** *4* (4), eaas8998

(11) Gupta, P. B.; Fillmore, C. M.; Jiang, G.; Shapira, S. D.; Tao, K.; Kuperwasser, C.; Lander, E. S. Stochastic state transitions give rise to phenotypic equilibrium in populations of cancer cells. *Cell* **2011,** *146* (4), 633–644

(12) Chaffer, C. L.; Brueckmann, I.; Scheel, C.; Kaestli, A. J.; Wiggins, P. A.; Rodrigues, L. O.; Brooks, M.; Reinhardt, F.; Su, Y.; Polyak, K.et al. Normal and neoplastic nonstem cells can spontaneously convert to a stem-like state. *Proc. Natl. Acad. Sci. U. S. A.* **2011,** *108* (19), 7950–7955

(13) Butcher, D. T.; Alliston, T.; Weaver, V. M. A tense situation: forcing tumour progression. *Nat. Rev. Cancer* **2009,** *9* (2), 108–122

(14) Tang, X.; Kuhlenschmidt, T. B.; Li, Q.; Ali, S.; Lezmi, S.; Chen, H.; Pires-Alves, M.; Laegreid, W. W.; Saif, T. A.; Kuhlenschmidt, M. S. A mechanically-induced colon cancer cell population shows increased metastatic potential. *Mol. Cancer* **2014,** *13*1

(15) Tan, Y.; Tajik, A.; Chen, J.; Jia, Q.; Chowdhury, F.; Wang, L.; Chen, J.; Zhang, S.; Hong, Y.; Yi, H.et al. Matrix softness regulates plasticity of tumour-repopulating cells via H3K9 demethylation and Sox2 expression. *Nat. Commun.* **2014,** *5*, 4619

(16) Liu, J.; Tan, Y.; Zhang, H.; Zhang, Y.; Xu, P.; Chen, J.; Poh, Y. C.; Tang, K.; Wang, N.; Huang, B. Soft fibrin gels promote selection and growth of tumorigenic cells. *Nat. Mater.* **2012,** *11* (8), 734–741

(17) Tan, Y.; Wood, A. R.; Jia, Q.; Zhou, W.; Luo, J.; Yang, F.; Chen, J.; Chen, J.; Sun, J.; Seong, J.et al. Soft matrices downregulate FAK activity to promote growth of tumor-repopulating cells. *Biochem. Biophys. Res. Commun.* **2017,** *483* (1), 456–462

(18) Yu, L.; Hou, Y.; Xie, W.; Camacho, J. L. C.; Cheng, C.; Holle, A.; Young, J.; Trappmann, B.; Zhao, W.; Melzig, M. F.et al. Ligand Diffusion Enables Force-Independent Cell Adhesion via Activating alpha5beta1 Integrin and Initiating Rac and RhoA Signaling. *Adv. Mater.* **2020,** *32* (29), e2002566.

(19) Yu, L.; Hou, Y.; Xie, W.; Cuellar-Camacho, J. L.; Wei, Q.; Haag, R. Self-Strengthening Adhesive Force Promotes Cell Mechanotransduction. *Adv. Mater.* **2020,** *32* (52), e2006986.

(20) Kang, H.; Wong, D. S. H.; Yan, X.; Jung, H. J.; Kim, S.; Lin, S.; Wei, K.; Li, G.; Dravid, V. P.; Bian, L. Remote Control of Multimodal Nanoscale Ligand Oscillations Regulates Stem Cell Adhesion and Differentiation. *ACS Nano* **2017,** *11* (10), 9636–9649

(21) Wong, D. S.; Li, J.; Yan, X.; Wang, B.; Li, R.; Zhang, L.; Bian, L. Magnetically Tuning Tether Mobility of Integrin Ligand Regulates Adhesion, Spreading, and Differentiation of Stem Cells. *Nano Lett.* **2017,** *17* (3), 1685–1695

(22) Kang, H.; Jung, H. J.; Wong, D. S. H.; Kim, S. K.; Lin, S.; Chan, K. F.; Zhang, L.; Li, G.; Dravid, V. P.; Bian, L. Remote Control of Heterodimeric Magnetic Nanoswitch Regulates the Adhesion and Differentiation of Stem Cells. *J. Am. Chem. Soc.* **2018,** *140* (18), 5909–5913

(23) Wong, S. H. D.; Yin, B. H.; Yang, B. G.; Lin, S. E.; Li, R.; Feng, Q.; Yang, H. R.; Zhang, L.; Yang, Z. M.; Li, G.et al. Anisotropic Nanoscale Presentation of Cell Adhesion Ligand Enhances the Recruitment of Diverse Integrins in Adhesion Structures and Mechanosensing-Dependent Differentiation of Stem Cells. *Adv. Funct. Mater.* **2019,** *29* (8), 1806822

(24) Wong, S. H. D.; Wong, W. K. R.; Lai, C. H. N.; Oh, J.; Li, Z.; Chen, X.; Yuan, W.; Bian, L. Soft Polymeric Matrix as a Macroscopic Cage for Magnetically Modulating Reversible Nanoscale Ligand Presentation. *Nano Lett.* **2020,** *20* (5), 3207–3216

(25) Yamaoka, T.; Tabata, Y.; Ikada, Y. Distribution and tissue uptake of poly(ethylene glycol) with different molecular weights after intravenous administration to mice. *J. Pharm. Sci.* **1994,** *83* (4), 601–606.

(26) Liu, Y.; Medda, R.; Liu, Z.; Galior, K.; Yehl, K.; Spatz, J. P.; Cavalcanti-Adam, E. A.; Salaita, K. Nanoparticle Tension Probes Patterned at the Nanoscale: Impact of Integrin Clustering on Force Transmission. *Nano Lett.* **2014,** *14* (10), 5539–5546.

(27) Jurchenko, C.; Chang, Y.; Narui, Y.; Zhang, Y.; Salaita, K. S. Integrin-generated forces lead to streptavidin-biotin unbinding in cellular adhesions. *Biophys J* **2014,** *106* (7), 1436.

(28) Li, S.; Bai, H.; Chen, X.; Gong, S.; Xiao, J.; Li, D.; Li, L.; Jiang, Y.; Li, T.; Qin, X.et al. Soft Substrate Promotes Osteosarcoma Cell Self-Renewal, Differentiation, and Drug Resistance Through miR-29b and Its Target Protein Spin 1. *ACS Biomater. Sci. Eng.* **2020,** *6* (10), 5588–5598.

(29) Chowdhury, F.; Li, Y.; Poh, Y. C.; Yokohama-Tamaki, T.; Wang, N.; Tanaka, T. S. Soft substrates promote homogeneous self-renewal of embryonic stem cells via downregulating cell-matrix tractions. *Plos One* **2010,** *5* (12), e15655.

(30) Trappmann, B.; Gautrot, J. E.; Connelly, J. T.; Strange, D. G.; Li, Y.; Oyen, M. L.; Cohen Stuart, M. A.; Boehm, H.; Li, B.; Vogel, V.et al. Extracellular-matrix tethering regulates stem-cell fate. *Nat. Mater.* **2012,** *11* (7), 642–649.

(31) Young, J. L.; Hua, X.; Somsel, H.; Reichart, F.; Kessler, H.; Spatz, J. P. Integrin Subtypes and Nanoscale Ligand Presentation Influence Drug Sensitivity in Cancer Cells. *Nano Lett.* **2020,** *20* (2), 1183–1191.

(32) Lozeau, L. D.; Alexander, T. E.; Camesano, T. A. Proposed Mechanisms of Tethered Antimicrobial Peptide Chrysophsin-1 as a Function of Tether Length Using QCM-D. *J. Phys. Chem. B* **2015,** *119* (41), 13142–13151.

(33) Attwood, S. J.; Cortes, E.; Haining, A. W. M.; Robinson, B.; Li, D. Y.; Gautrot, J.; Hernandez, A. D. Adhesive ligand tether length affects the size and length of focal adhesions and influences cell spreading and attachment. *Sci. Rep.* **2016,** *6, 34334*.

(34) Liu, Y.; Medda, R.; Liu, Z.; Galior, K.; Yehl, K.; Spatz, J. P.; Cavalcanti-Adam, E. A.; Salaita, K. Nanoparticle Tension Probes Patterned at the Nanoscale: Impact of Integrin Clustering on Force Transmission. *Nano Lett.* **2014,** *14* (10), 5539–5546.

(35) Chen, S. F.; Chang, Y. C.; Nieh, S.; Liu, C. L.; Yang, C. Y.; Lin, Y. S. Nonadhesive culture system as a model of rapid sphere formation with cancer stem cell properties. *Plos One* **2012,** *7* (2), e31864.

(36) Mitjans, F.; Sander, D.; Adan, J.; Sutter, A.; Martinez, J. M.; Jaggle, C. S.; Moyano, J. M.; Kreysch, H. G.; Piulats, J.; Goodman, S. L. An anti-alpha-v-integrin antibody that blocks integrin function inhibits the development of a human-melanoma in nude-mice. *J. Cell Sci.*

1995, *108*, 2825–2838.

(37) Chowdhury, F.; Doganay, S.; Leslie, B. J.; Singh, R.; Amar, K.; Talluri, B.; Park, S.; Wang, N.; Ha, T. Cdc42-dependent modulation of rigidity sensing and cell spreading in tumor repopulating cells. *Biochem. Bioph. Res. Co.* **2018,** *500* (3), 557–563.

(38) Zhou, Y.; Song, N.; Li, X.; Han, Y.; Ren, Z.; Xu, J. X.; Han, Y. C.; Li, F.; Jia, X. Changes in the methylation status of the Oct3/4, Nanog, and Sox2 promoters in stem cells during regeneration of rat tracheal epithelium after injury. *Oncotarget* **2017,** *8* (2), 2984–2994.

(39) Champeris Tsaniras, S.; Kanellakis, N.; Symeonidou, I. E.; Nikolopoulou, P.; Lygerou, Z.; Taraviras, S. Licensing of DNA replication, cancer, pluripotency and differentiation: an interlinked world? *Semin. Cell Dev. Biol.* **2014,** *30*, 174–180.

(40) Raab-Westphal, S.; Marshall, J. F.; Goodman, S. L. Integrins as therapeutic targets: successes and cancers. *Cancers* **2017,** *9* (9), 110.

(41) Wang, K.; Zeng, J.; Luo, L.; Yang, J.; Chen, J.; Li, B.; Shen, K. Identification of a cancer stem cell-like side population in the HeLa human cervical carcinoma cell line. *Oncol. Lett.* **2013,** *6* (6), 1673–1680.

(42) Wang, J.; Wu, Y.; Gao, W.; Li, F.; Bo, Y.; Zhu, M.; Fu, R.; Liu, Q.; Wen, S.; Wang, B. Identification and characterization of CD133(+)CD44(+) cancer stem cells from human laryngeal squamous cell carcinoma cell lines. *J. Cancer* **2017,** *8* (3), 497–506.

(43) Zhang, X.; Hua, R.; Wang, X.; Huang, M.; Gan, L.; Wu, Z.; Zhang, J.; Wang, H.; Cheng, Y.; Li, J.et al. Identification of stem-like cells and clinical significance of candidate stem cell markers in gastric cancer. *Oncotarget* **2016,** *7* (9), 9815–9831.

(44) Jeter, C. R.; Liu, B.; Liu, X.; Chen, X.; Liu, C.; Calhoun-Davis, T.; Repass, J.; Zaehres, H.; Shen, J. J.; Tang, D. G. NANOG promotes cancer stem cell characteristics and prostate cancer resistance to androgen deprivation. *Oncogene* **2011,** *30* (36), 3833–3845.

(45) Vazquez-Iglesias, L.; Barcia-Castro, L.; Rodriguez-Quiroga, M.; Paez de la Cadena, M.; Rodriguez-Berrocal, J.; Cordero, O. J. Surface expression marker profile in colon cancer cell lines and sphere-derived cells suggests complexity in CD26(+) cancer stem cells subsets. *Biol. Open* **2019,** *8* (7), bio041673.

(46) Cocconi, G.; Carlini, P.; Gamboni, A.; Gasperoni, S.; Rodino, C.; Zironi, S.; Bisagni, G.; Porrozzi, S.; Cognetti, F.; Di Costanzo, F.et al. Cisplatin, epirubicin, leucovorin and 5-fluorouracil (PELF) is more active than 5-fluorouracil, doxorubicin and methotrexate (FAMTX) in advanced gastric carcinoma. *Ann. Oncol.* **2003,** *14* (8), 1258–1263.

(47) Jing, C.; Cao, H.; Qin, X.; Yu, S.; Wu, J.; Wang, Z.; Ma, R.; Feng, J. Exosome-mediated gefitinib resistance in lung cancer HCC827 cells via delivery of miR-21. *Oncol. Lett.* **2018,** *15* (6), 9811–9817.

(48) Dean, M.; Hamon, Y.; Chimini, G. The human ATP-binding cassette (ABC) transporter

superfamily. *J. Lipid Res.* **2001,** *42* (7), 1156–1166.

(49) Tan, B.; Piwnica-Worms, D.; Ratner, L. Multidrug resistance transporters and modulation. *Curr. Opin. Oncol.* **2000,** *12* (5), 450–458

(50) Feng, Q.; Liu, J.; Li, X.; Chen, Q.; Sun, J.; Shi, X.; Ding, B.; Yu, H.; Li, Y.; Jiang, X. One-Step Microfluidic Synthesis of Nanocomplex with Tunable Rigidity and Acid-Switchable Surface Charge for Overcoming Drug Resistance. *Small* **2017,** *13* (9), 1603109.

(51) Yang, C.; Tibbitt, M. W.; Basta, L.; Anseth, K. S. Mechanical memory and dosing influence stem cell fate. *Nat. Mater.* **2014,** *13* (6), 645–652.

(52) Nasrollahi, S.; Walter, C.; Loza, A. J.; Schimizzi, G. V.; Longmore, G. D.; Pathak, A. Past matrix stiffness primes epithelial cells and regulates their future collective migration through a mechanical memory. *Biomater.* **2017,** *146*, 146–155.

(53) Boia-Ferreira, M.; Basilio, A. B.; Hamasaki, A. E.; Matsubara, F. H.; Appel, M. H.; Costa, C. R. V.; Amson, R.; Telerman, A.; Chaim, O. M.; Veiga, S. S.et al. TCTP as a therapeutic target in melanoma treatment. *Br. J. Cancer* **2017,** *117* (5), 656–665.

(54) Apostolopoulos, V.; Xing, P. X.; McKenzie, I. F. Murine immune response to cells transfected with human MUC1: immunization with cellular and synthetic antigens. *Cancer Res.* **1994,** *54* (19), 5186–5193.

(55) Wang, C.; Sun, W.; Ye, Y.; Hu, Q.; Bomba, H. N.; Gu, Z. *In situ* activation of platelets with checkpoint inhibitors for post-surgical cancer immunotherapy. *Nat. Biomed. Eng.* **2017,** *1* (2), 0011.

(56) Chao, Y.; Liang, C.; Tao, H. Q.; Du, Y. R.; Wu, D.; Dong, Z. L.; Jin, Q. T.; Chen, G. B.; Xu, J.; Xiao, Z. S.et al. Localized cocktail chemoimmunotherapy after in situ gelation to trigger robust systemic antitumor immune responses. *Sci. Adv.* **2020,** *6* (10), eaaz4204.

(57) Zhong, F.; Cheng, X.; Sun, S.; Zhou, J. Transcriptional activation of PD-L1 by Sox2 contributes to the proliferation of hepatocellular carcinoma cells. *Oncol. Rep.* **2017,** *37* (5), 3061–3067.

(58) Garcia-Diaz, A.; Shin, D. S.; Moreno, B. H.; Saco, J.; Escuin-Ordinas, H.; Rodriguez, G. A.; Zaretsky, J. M.; Sun, L.; Hugo, W.; Wang, X.et al. Interferon receptor signaling pathways regulating PD-L1 and PD-L2 expression. *Cell Rep.* **2017,** *19* (6), 1189–1201.

(59) Su, W. H.; Chuang, P. C.; Huang, E. Y.; Yang, K. D. Radiation-induced increase in cell migration and metastatic potential of cervical cancer cells operates via the K-Ras pathway. *Am. J. Pathol.* **2012,** *180* (2), 862–71.

(60) Codony-Servat, J.; Rosell, R. Cancer stem cells and immunoresistance: clinical implications and solutions. *Transl. Lung Cancer Res.* **2015,** *4* (6), 689–703.

Groups of fabricated surfaces	The average molecular weight of PEG linker (DA)	Magnetic application	Group name abbreviation
Low tether mobility	2000	–	MNP2k–M
Medium tether mobility	5000	–	MNP5k–M
High tether mobility	20000	–	MNP20k–M
Restricted tether mobility	2000	+	MNP2k+M
Restricted tether mobility	5000	+	MNP5k+M
Restricted tether mobility	20000	+	MNP20k+M
The symbols "+" and "–" present in the column "Magnetic Application" indicate that these two items are present or absent.			

Table 1. Group name abbreviation of all groups in the study (MNP: magnetic nanoparticle)

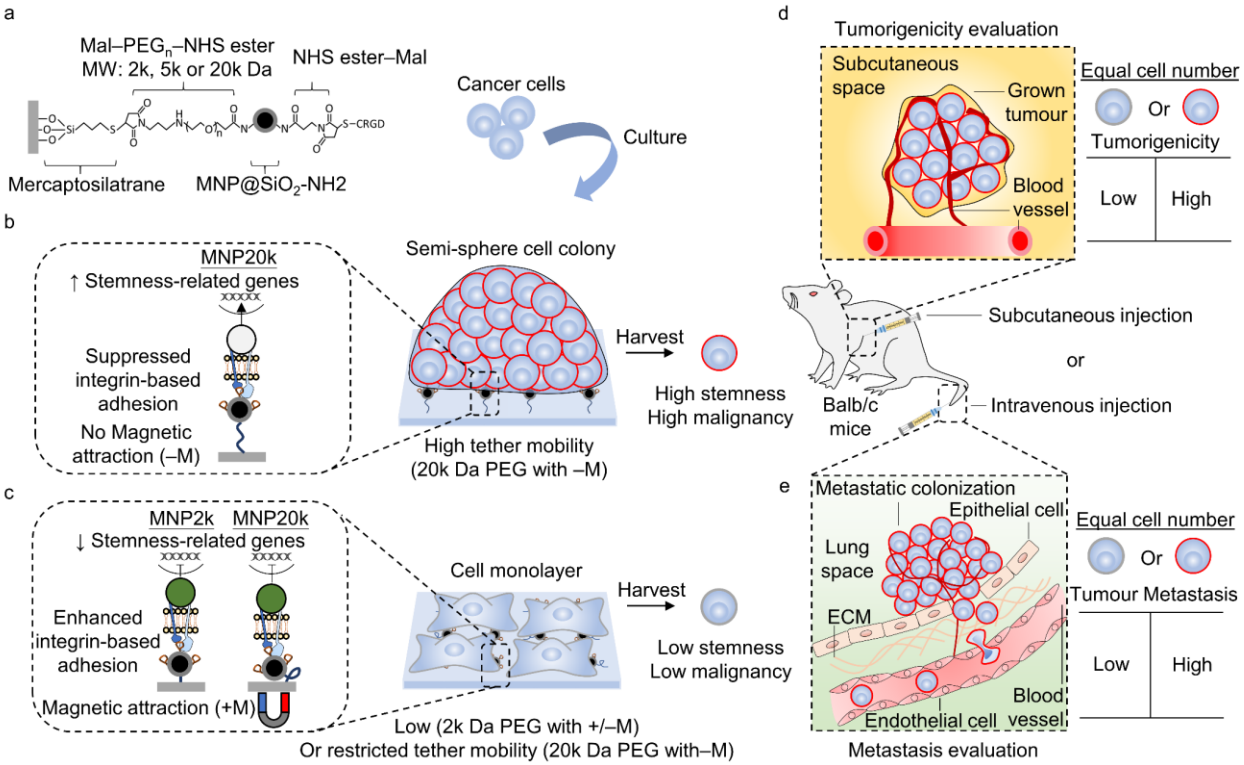

Scheme 1. Schematic illustration of the magnetic-responsive platform and experimental design to manipulate ligand presentation to culture cancer cells with enhanced stemness. (a) Detailed chemical structure of the RGD-bearing magnetic nanoparticles (RGD-MNPs) conjugated on the glass substrate via a flexible and non-fouling poly(ethylene) glycol (PEG) linker with various molecular weights (2k, 5k and 20k Da) to control the nanoscale tether mobility of integrin-ligand binding. (b) The hypothetical schematic drawing shows that the PEG linker of large molecular weight (20k Da) elevates the nanoscale tether mobility of the integrin ligand RGD, (c) which can be instantaneously reduced upon switching on the downward magnetic attraction (+M). Such tunable tether mobility of the integrin ligand can influence the mechanotransduction signalling and the associated epigenetic events of seeded cancer cells, leading to alteration of the stemness of cancer cells. The cancer cells with a high degree of stemness obtained from culturing on the substrate with a high-mobility ligand tether showed significantly increased (d) tumorigenicity and (e) metastasis *in vivo* after being delivered via subcutaneous and intravenous injections, respectively.

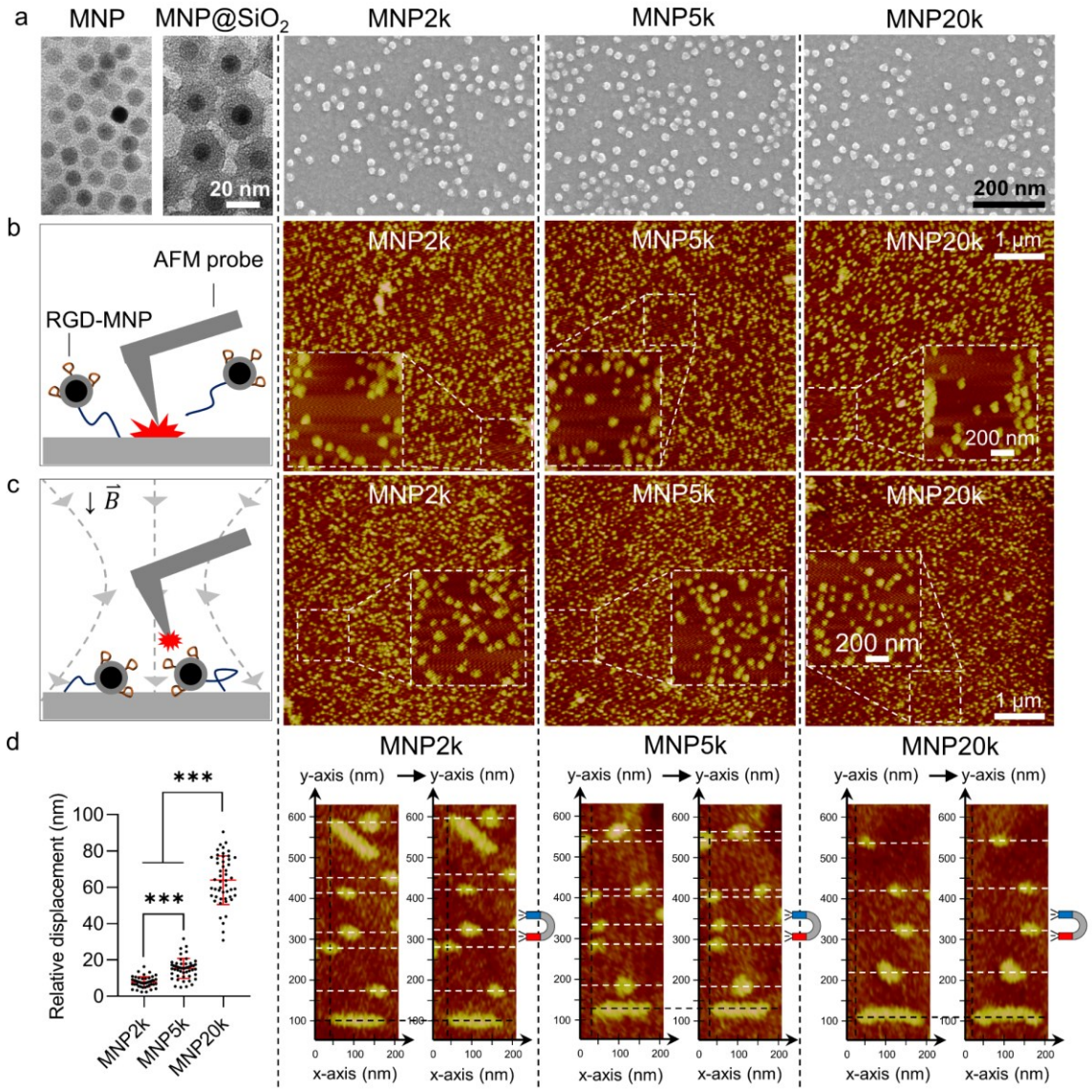

Figure 1. Dynamic characterization of the nanoscale tether mobility of RGD-MNPs. (a) Nanoscopic characterization of MNP and MNP@SiO_2 by transmission electron micrographs (TEM) and scanning electron microscopy (SEM) images of the RGD-MNP tethered onto a glass substrate via a PEG linker with varying molecular weights (2k, 5k and 20k). Schematic illustration and atomic force microscopy (AFM) characterization of the RGD-MNP tether stability (b) without (–M) or (c) with downward magnetic attraction (+M). (d) Quantification of the relative displacement of the RGD-MNPs tethered with PEG linkers of varying molecular weights in response to lateral magnetic attraction by AFM. The black dotted lines were used as the reference coordinates (immobilized gold nanorods), and the white dotted lines were drawn across the centre coordinate of each RGD-MNP. The error bars represent the s.e.m., each point representing a particle displacement (n = 50) from three different substrates. Significant difference p-value:

***<0.001. (one-way ANOVA)

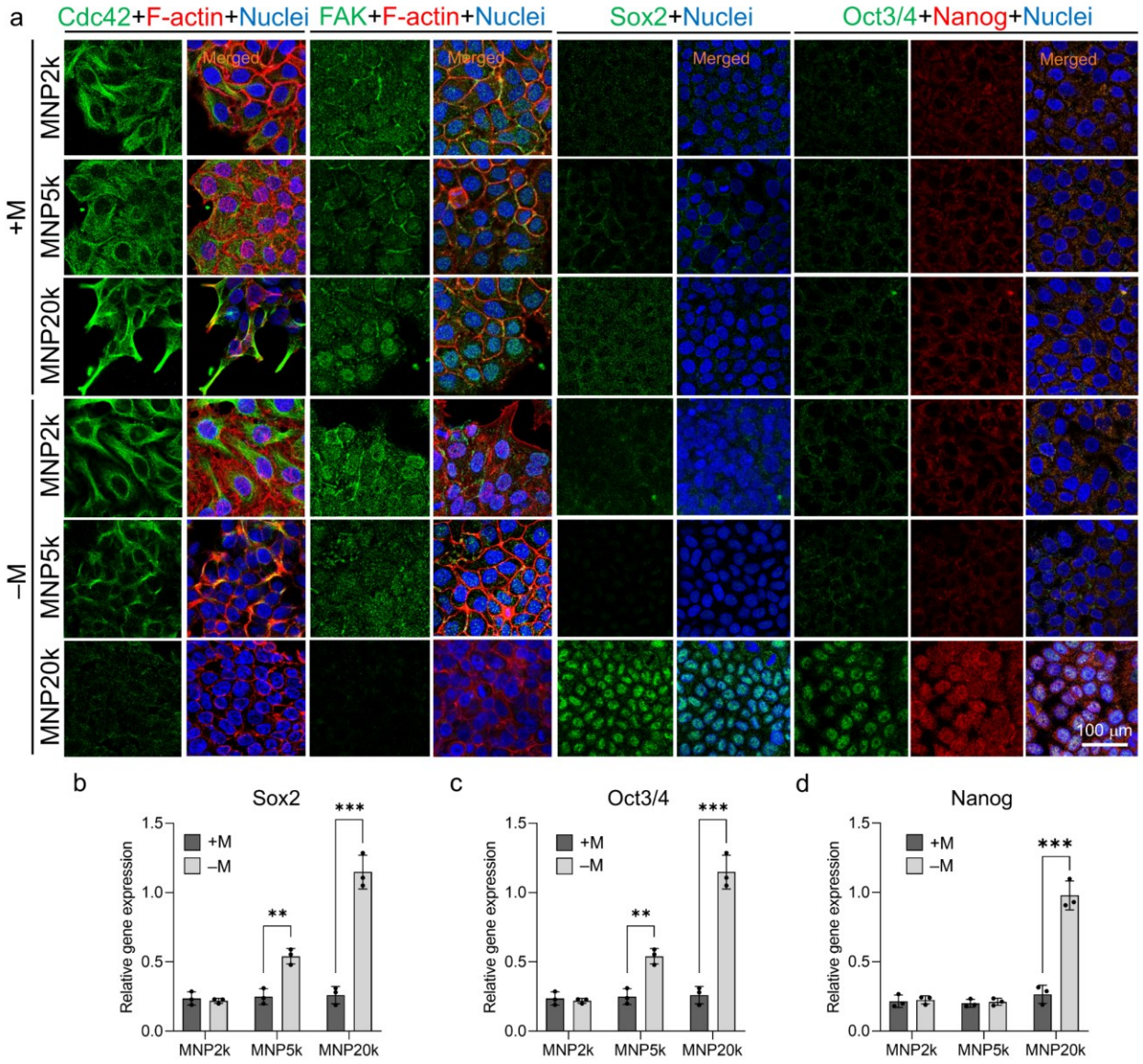

Figure 2. Magnetic tuning of the cell adhesive ligand presentation regulates mechanotransduction signalling, epigenetics, and expression of stemness markers in cancer cells. (a) Immunofluorescence staining of cdc42 (green), FAK (green), Sox2 (green), Oct3/4 (green), and Nanog (red) together with cytoskeleton F-actin (red) and nuclei (blue) in HeLa cells cultured under –M or +M conditions. Relative gene expression levels of (b) Sox2, (c) Oct3/4, and (d) Nanog in HeLa cells from different groups (n=3, each point represents one independent substrate), where these genes were normalized to the housekeeping gene GAPDH. Data are all shown as the mean±s.d., significant difference p-value: **<0.01 and ***<0.001. (one-way ANOVA)

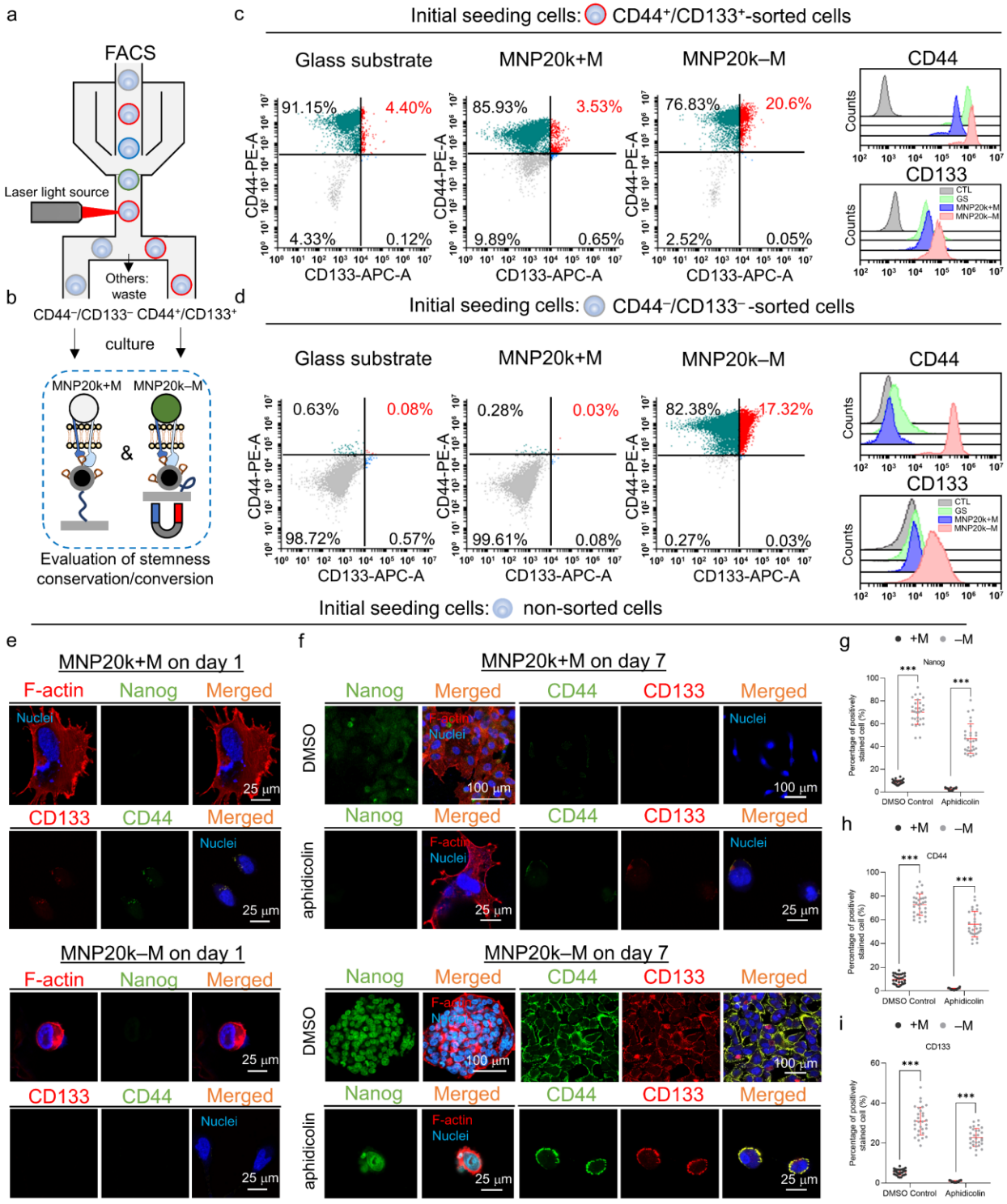

Figure 3. The substrate with high tether mobility of cell adhesive ligand enhances the expression of cancer stem-like cell surface markers in cultured HeLa cells. (a) Schematic illustration showing fluorescence-activated cell sorting (FACS) of $CD44^{-}/CD133^{-}$ or $CD44^{+}/CD133^{+}$ cells from a population of HeLa cells cultured on a cell culture plate and (b) the

subsequent culture of the sorted cells on MNP20k–/+M substrates. Dot plots and histogram representations of the CD44 and CD133 expression of (c) the $CD44^{+}/CD133^{+}$-sorted cells and (d) the $CD44^{-}/CD133^{-}$-sorted cells after 7 days of culture on the glass, MNP20k+M, and MNP20k–M substrates, respectively. CTL and GS represent unstained control and the glass substrate, respectively. Immunofluorescence staining of Sox2 (green), CD44 (green) and CD133 (red) in the entire population (non-sorted) of HeLa cells cultured on the MNP20k–/+M substrates (e) for 1 day followed by (f) 6 additional days of culture with medium supplemented with DMSO/aphidicolin drug for 7 days. (g-i) Statistical analysis of positively stained cells in each group (n=30 randomly selected microscopy view areas of identical size from three different substrates, each point represents one area) for the expression of Nanog, CD44 and CD133. Data are all shown as the mean±s.d., significant difference p-value: **<0.01 and ***<0.001. (one-way ANOVA)

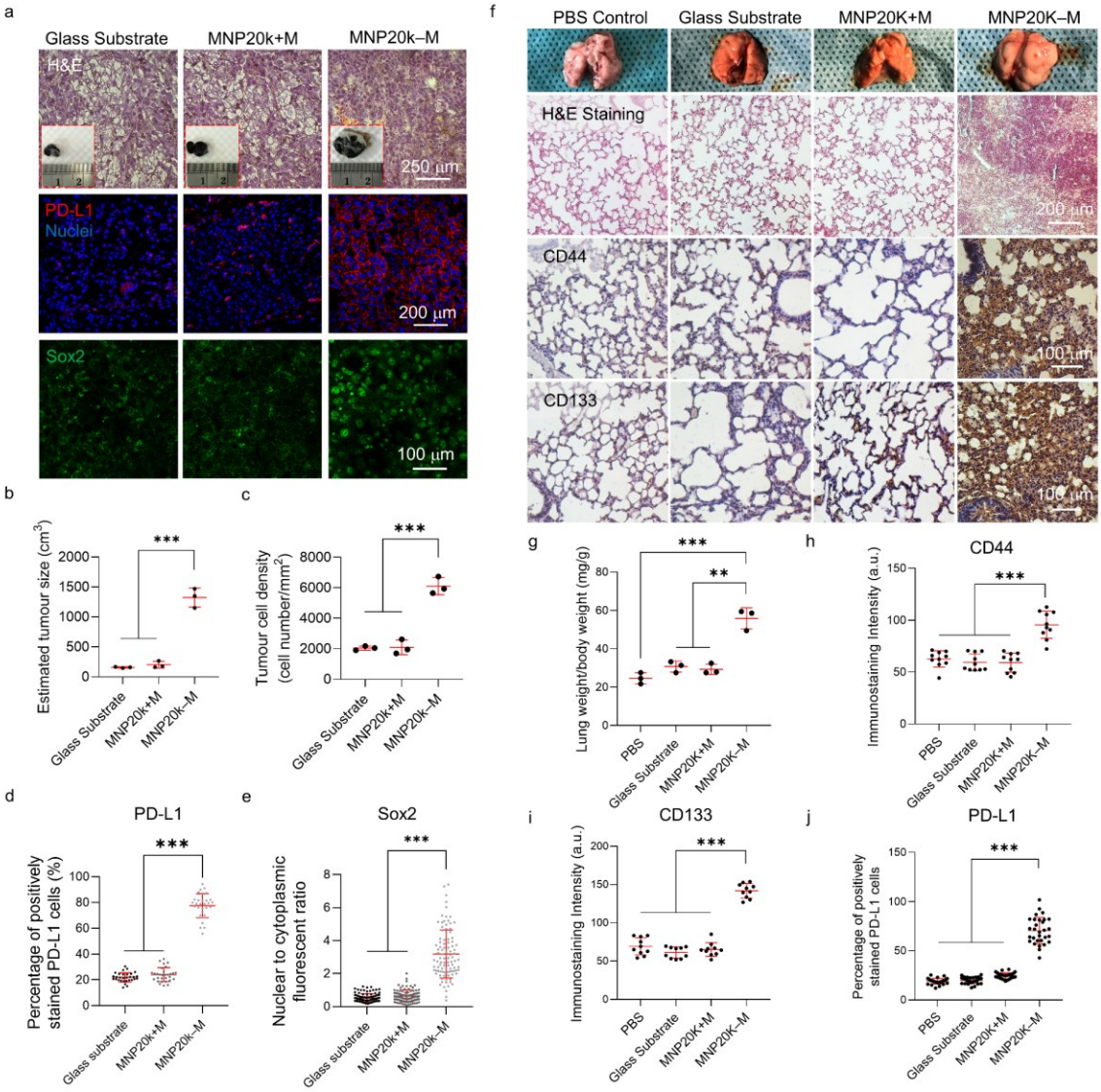

Figure 4. B16-F1 cells and HeLa cells cultured on substrates with high ligand tether mobility show dramatically enhanced tumorigenicity and metastatic potential, respectively, in BALB/c mice. The mice were subcutaneously (B16-F1) or intravenously injected (HeLa cells) the harvested cells (10^5 cells) from substrates with varying ligand tether mobilities after 7 days of culture. (a) Images of B16-F1 solid tumours (inlet images) formed in different groups 2 weeks after injection of cells with hematoxylin and eosin (H&E) staining and immunofluorescence staining of inhibitory immune checkpoint ligand (PD-L1, red) and stemness marker, Sox2 (green). Statistical quantification of (b) tumour size (n=3), (c) tumour cell density (n=3), (d) the percentage of PD-L1-positive cells in the tumour samples (n=30 randomly selected microscopy view areas of identical size from three different tumours). (e) Nuclear localization of Sox2 in solid tumours (n=100 cells from 3 different tumours). (f) Images of the lungs extracted 1-month after injection of cells with H&E staining and immunostaining of CD44 and CD133. Statistical quantification of

(g) the weight of extracted lungs normalized by body weight (n=3), immunostaining intensity of (h) CD44 and (i) CD133 (n=10 sections from 3 different lung samples), and (j) the percentage of PD-L1 positive cells in the lung samples (n=30 randomly selected microscopic areas of identical size from three different substrates). Data are all shown as the mean±s.d., with each point representing one cell from the images or one tumour sample from mice. Significant difference, p-value: ***<0.001. (one-way ANOVA)

TOC Graphic

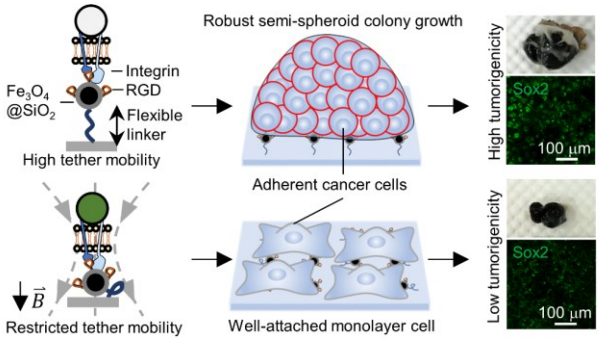
Integrin
RGD
Fe_3O_4 @SiO_2
Flexible linker
High tether mobility
$\vec{B}$
Restricted tether mobility
Robust semi-spheroid colony growth
Adherent cancer cells
Well-attached monolayer cell
High tumorigenicity
Low tumorigenicity
Sox2
100 μm
Sox2
100 μm